HIGH-RESOLUTION DOA ESTIMATION USING SINGLE-SNAPSHOT MUSIC FOR AUTOMOTIVE RADAR WITH MIXED-ADC ALLOCATIONS

Moritz Kahlert[†], *Lifan Xu*[‡], *Tai Fei*[§], *Markus Gardill*[⋆], *and Shunqiao Sun*[‡]

[†]HELLA GmbH & Co. KGaA, Lippstadt, Germany
[§]University of Applied Sciences and Arts, Dortmund, Germany
[⋆]Brandenburg University of Technology, Cottbus, Germany
[‡]Department of Electrical and Computer Engineering, University of Alabama, Tuscaloosa, AL, USA

2024 IEEE 13th Sensor Array and Multichannel Signal Processing Workshop (SAM) | 979-8-3503-4481-3/24/$31.00 ©2024 IEEE | DOI: 10.1109/SAM60225.2024.10636418

ABSTRACT

Fine direction of arrival (DOA) estimations are required for accurate target detections in automotive radar systems. To address this issue, most spectral estimation methods assume many snapshots of measurements. However, due to the dynamic nature of automotive scenarios, methods using multiple snapshots are impractical for DOA estimation in automotive radars. Furthermore, to relax the hardware requirements on modern automotive radar systems, mixed-analog-to-digital converter (ADC) allocations, i.e., the coexistence of 1-bit and high-resolution ADCs, have gained more attention recently. In this work, we introduce a high-resolution DOA estimation approach based on single-snapshot multiple signal classification (MUSIC) estimation and evaluate the performance with various ADC allocations. The results show that mixed-ADC allocations can perform comparably to high-resolution ADC allocations.

***Index Terms*—automotive radar, direction of arrival estimation, mixed ADCs, single-snapshot MUSIC**

I. INTRODUCTION

Automotive radar operating at millimeter-wave frequency, i.e., 76-81 GHz, plays an important role in autonomous driving systems due to its robustness in environment perception under all weather conditions [1], [2]. Existing automotive radar transceivers, such as NXP Semiconductors MR3003 and Texas Instruments AWR1243 [3], support up to 3 transmit and 4 receive antennas, yielding an angular resolution of around 10°, which is not capable for Level 4 and Level 5 autonomous driving where a vehicle drives itself in all conditions without any human interaction.

Recent advances in waveform design, particularly the integration of digital modulation schemes like phase-modulated continuous wave (PMCW) [4], have paved the way for innovative solutions. Among them, the adoption of massive multiple input multiple output (MIMO) technology has been proposed, complemented by high-resolution direction of arrival (DOA) algorithms. This approach aims to enhance angular resolution and separability in intricate automotive scenarios. Estimating the DOA is a crucial task in automotive radar systems. Traditional subspace-based algorithms for DOA estimation, like multiple signal classification (MUSIC) [5] and estimation of signal parameters via rotational invariant techniques (ESPRIT) [6], depend on multiple snapshots to achieve precise DOA estimates. However, the rapidly changing nature of automotive environments often allows for only a limited number of radar snapshots, or in some cases, just a single snapshot for DOA estimation. It is of great importance to develop single-snapshot DOA estimation methods for automotive radars. Recent advances in high-resolution single-snapshot DOA estimation include iterative adaptive approach (IAA) [7], [8], compressive sensing [9]–[12], single-snapshot MUSIC [13], data-driven deep neural networks [14], and model-based unrolling neural networks [15], [16]. Moreover, the stringent demands on analog-to-digital converters (ADCs) and the storage in digital modulation with broad bandwidth have sparked interest in incorporating low-resolution ADCs, including extreme cases like 1-bit ADCs [17], into the system design. This strategic integration will render the system viable for widespread civil deployment in massive autonomous driving applications. The application of the arcsine law (refer to page 396 in [18]) facilitates the estimation of the covariance matrix, a prerequisite for high-resolution algorithms such as those discussed in [19]. Nevertheless, the dynamic nature of automotive scenarios introduces significant challenges, making estimating the covariance matrix over multiple snapshots nearly impractical [1].

In this work, we introduce a novel high-resolution DOA estimation approach involving a uniform linear array (ULA) with a mixed-ADC solution based on a single snapshot. This entails the coexistence of both high-resolution and 1-bit ADCs within the system. We present a single-snapshot-based MUSIC technique utilizing the Hankel matrix and singular value decomposition (SVD) [13]. This innovative method is developed to address and resolve the DOA in radar systems with mixed-ADC allocations. In addition, we evaluate the performance of different allocations with extensive simulations.

The work of L. Xu and S. Sun was supported in part by U.S. National Science Foundation (NSF) under Grant CCF-2153386.

II. SYSTEM MODEL

Consider a ULA consisting of M antenna elements with half-wavelength, i.e., $\lambda/2$, inter-element spacing. These elements receive narrowband far-field signals from K different directions θ_k with $k \in \{1, \ldots, K\}$. Then, the sampled signal in the single snapshot case can be expressed by

$$\mathbf{x} = \mathbf{A}^{M}(\boldsymbol{\theta})\,\mathbf{s} + \mathbf{n}, \tag{1}$$

where the vector $\mathbf{x} = [x_1, \ldots, x_M]^{\mathsf{T}} \in \mathbb{C}^{M\times 1}$ contains the sampled array measurements, $\mathbf{A}^{M}(\boldsymbol{\theta}) = [\mathbf{a}(\theta_1), \ldots, \mathbf{a}(\theta_K)] \in \mathbb{C}^{M\times K}$ is the steering matrix with steering vectors $\mathbf{a}^{M}(\theta_k) = \big[1, \exp\big(\jmath\pi \sin(\theta_k)\big), \ldots, \exp\big(\jmath\pi(M-1)\sin(\theta_k)\big)\big]^{\mathsf{T}} \in \mathbb{C}^{M\times 1}$ and angles $\boldsymbol{\theta} = [\theta_1, \ldots, \theta_K] \in \mathbb{R}^{K\times 1}$, $\mathbf{s} = [s_1, s_2, \ldots, s_K]^{\mathsf{T}} \in \mathbb{C}^{K\times 1}$ is the source signal vector, $\mathbf{n} = [n_1, n_2, \ldots, n_M]^{\mathsf{T}} \in \mathbb{C}^{M\times 1}$ is a noise vector with complex-valued white Gaussian distributed values, $(\cdot)^{\mathsf{T}}$ is the transpose operation, $\jmath = \sqrt{-1}$ is the imaginary unit, and bold lowercase symbols indicate vectors and bold uppercase symbols matrices. For the sake of simplicity, in the following $\mathbf{A}$ and $\mathbf{a}$ are used instead of $\mathbf{A}(\theta)$ and $\mathbf{a}(\theta)$ without losing generality.

II-A. Mixed-ADC allocation

Further, we assume that the signals in the $M = M_0 + M_1$ elements are sampled by high-resolution or 1-bit ADCs, where $M_0 \in \mathbb{N}_0$ denotes the number of high-resolution and $M_1 \in \mathbb{N}_0$ the number of 1-bit ADCs in the system. When a 1-bit ADC is used at the m th antenna element, the quantized signal at the output of the ADC can be expressed as

$$z_m = \mathcal{Q}(x_m - h) = \operatorname{sgn}\big(\Re(x_m - h)\big) + \jmath \operatorname{sgn}\big(\Im(x_m - h)\big), \tag{2}$$

where $\mathcal{Q}(\cdot) = \operatorname{sgn}\big(\Re(\cdot)\big) + \jmath\operatorname{sgn}\big(\Im(\cdot)\big)$ is the complex quantization operation, $\Re(\cdot)$ and $\Im(\cdot)$ are the real- and imaginary parts, respectively, h is a time-varying known threshold, and $\operatorname{sgn}(\cdot)$ is the signum function, that is defined as

$$\operatorname{sgn}(\mathbf{x}) = \begin{cases} -1 & \text{if } x < 0 \\ 1 & \text{if } x \geq 0. \end{cases} \tag{3}$$

Then, in a mixed-ADC system, i.e., the coexistence of high-resolution and 1-bit ADCs, the sampled signal can be expressed by

$$\mathbf{y} = \mathbf{x} \circ \boldsymbol{\delta} + \mathbf{z} \circ \bar{\boldsymbol{\delta}}, \tag{4}$$

where $\mathbf{y} = [y_1, \ldots, y_M]^{\mathsf{T}} \in \mathbb{C}^{M\times 1}$ with $y_m \in \{x_m, z_m\}$, $\boldsymbol{\delta} = [\delta_1, \ldots, \delta_M]^{\mathsf{T}} \in \mathbb{C}^{M\times 1}$ with $\delta_m \in \{0, 1\}$ defines the allocation of high-resolution and 1-bit ADCs to the M antenna elements, and $\circ$ denotes the Hadamard product, i.e., the element-wise product. $\delta_m = 0$ indicates the allocation of a 1-bit ADC at the mth antenna element, and $\delta_m = 1$ the allocation of a high-resolution ADC. Further $\bar{\boldsymbol{\delta}}$ is defined as $\bar{\boldsymbol{\delta}} = \mathbf{1}_M - \boldsymbol{\delta}$ with $\mathbf{1}_M = [1, 1, \ldots, 1]^{\mathsf{T}} \in \mathbb{R}^{M\times 1}$, and it holds that $1_M^{\mathsf{T}}\boldsymbol{\delta} = M_0$ and $\mathbf{1}_M^{\mathsf{T}}\bar{\boldsymbol{\delta}} = M_1$.

II-B. Single-Snapshot MUSIC

Like other spectral estimation decomposition methods, MUSIC typically requires multiple snapshots to calculate the covariance matrix. However, the dynamic nature of automotive scenarios makes collecting multiple snapshots impractical. To address this issue, we consider a single snapshot spectral estimation approach based on the Hankel matrix introduced in [13]. This method can be viewed as a spatial smoothing technique specifically designed for ULA. Based on the sampled mixed-ADC output in (4), the Hankel matrix $\mathbf{H} \in \mathbb{C}^{(L+1)\times(M-L)}$ can be expressed as

$$\mathbf{H} = \operatorname{Hankel}(\mathbf{y}) = \begin{bmatrix} y_1 & y_2 & \cdots & y_{M-L} \\ y_2 & y_3 & \cdots & y_{M-L+1} \\ \vdots & \vdots & \ddots & \vdots \\ y_{L+1} & y_{L+2} & \cdots & y_M \end{bmatrix}, \tag{5}$$

where $1 \leq L < M$. The SVD of $\mathbf{H}$ results in

$$\mathbf{H} = \underbrace{[\mathbf{U}_{\mathrm{s}}, \mathbf{U}_{\mathrm{n}}]}_{\mathbf{U}}\ \underbrace{\operatorname{diag}(\sigma_1, \sigma_2, \ldots, \sigma_s, \sigma_{s+1}, \ldots)}_{\boldsymbol{\Sigma}}\ \underbrace{[\mathbf{V}_1, \mathbf{V}_2]^{\mathsf{H}}}_{\mathbf{V}^{\mathsf{H}}}, \tag{6}$$

where the columns of the square matrix $\mathbf{U} \in \mathbb{C}^{(L+1)\times(L+1)}$ with $\mathbf{U}_{\mathrm{s}} \in \mathbb{C}^{(L+1)\times s}$ and $\mathbf{U}_{\mathrm{n}} \in \mathbb{C}^{(L+1)\times(L+1-s)}$ are the signal and noise spaces, respectively, the diagonal matrix $\boldsymbol{\Sigma} \in \mathbb{C}^{(L+1)\times(M-L)}$ contains the eigenvalues with $\sigma_1 \geq \sigma_2 \geq \sigma_3 \geq \ldots$, the columns of $\mathbf{V} \in \mathbb{C}^{(M-L)\times(M-L)}$ with $\mathbf{V}_1 \in \mathbb{C}^{(M-L)\times s}$ and $\mathbf{V}_2 \in \mathbb{C}^{(M-L)\times(M-L-s)}$ are the right singular vectors, s is the number of potential target angles, and $(\cdot)^{\mathsf{H}}$ denotes the Hermitian transpose. The parameter L defines can be selected between 1 and M. The choice of L is discussed in Section III.

To estimate the DOAs, the steering vectors $\mathbf{a}^{L+1}(\theta_k)$ that are orthogonal to the noise subspace must be identified, i.e., $\mathbf{U}_{\mathrm{n}}^{\mathsf{H}}\boldsymbol{a}^{L+1}(\theta_k) = \mathbf{0}$, where $\mathbf{0} = [0, \ldots, 0]^{\mathsf{T}} \in \mathbb{R}^{(L+1-s)\times 1}$. The DOAs can be identified with θ_k corresponding to the s largest local maxima of the pseudospectrum

$$\mathbf{P}(\boldsymbol{\theta}) = \frac{\left\|\boldsymbol{a}^{L+1}\right\|_2}{\left\|\mathbf{U}_{\mathrm{n}}^{\mathsf{H}}\boldsymbol{a}^{L+1}\right\|_2}, \tag{7}$$

where $\|\cdot\|_2$ is the 2-norm, and $\mathbf{a}^{L+1}(\theta_k) = \big[1, \exp\big(\jmath\pi\sin(\theta_k)\big), \ldots, \exp\big(\jmath\pi L\sin(\theta_k)\big)\big]^{\mathsf{T}} \in \mathbb{C}^{(L+1)\times 1}$ is the steering vector at the angle θ_k.

II-C. CRB for Mixed-ADC Data

The authors in [20] derived the Cramer-Rao bound (CRB) for ULAs employing mixed-ADC allocations. For a single-snapshot single-target scenario, the CRB for θ_k can be calculated as

$$\operatorname{CRB}(\theta_k) = \frac{M_0 + \frac{2}{\pi}M_1}{2\pi^2 S}\,\frac{1}{\operatorname{SNR}\cos^2(\theta_k)}, \tag{8}$$

where $\mathrm{SNR} = p/\sigma^2$ is the signal-to-noise ratio (SNR) with the signal power p, and noise variance σ^2. The factor S is calculated as

$$S = \sum_{i=1}^{M} g_i (i-1)^2 \sum_{i=1}^{M} g_i - \left[\sum_{i=1}^{M} g_i (i-1)\right]^2, \quad (9)$$

where $\sum_{i=1}^{M} g_i = M_0 + \frac{2}{\pi} M_1$ with $g_i \in \left\{1, \frac{2}{\pi}\right\}$. While the SNR and the target parameters are fixed, the only value that can be optimized is S. The greater S, the lower becomes the CRB. S depends on the allocation of high and 1-bit ADCs to the antenna elements. Therefore, the CRB varies depending on the chosen ADC allocation and selecting the mixed-ADC allocation that minimizes CRB is desired.

II-D. MUSIC Error Variance

According to equation (7.5a) in [21], the MUSIC error variance is a function of σ^2, $\mathbf{R_{ss}}$, and θ_k and can be calculated as

$$\mathrm{var}\left(\hat{\theta}_k\right) = \frac{\sigma^2}{2N}\left\{\left[\mathbf{R_{ss}^{-1}}\right]_{kk} + \sigma^2\left[\mathbf{R_{ss}^{-1}}\left(\mathbf{A}^{\mathsf{H}}\mathbf{A}\right)^{-1}\mathbf{R_{ss}^{-1}}\right]_{kk}\right\}\frac{1}{h(\theta_k)}, \quad (10)$$

where σ^2 is the noise variance according to the definition in [21], $\mathbf{R_{ss}} = \mathbf{E}[\mathbf{s}\mathbf{s}^*]$ is the signal covariance matrix, $[\cdot]_{kk}$ denotes the (k,k)th element of the corresponding matrix, $\hat{\theta}_k$ is the estimated angle of the kth target, $N = M - L$ for the single-snapshot case, and

$$\mathbf{h}(\theta) = \mathbf{d}_\theta^{\mathsf{H}}\left[\mathbf{I} - \mathbf{A}(\mathbf{A}^{\mathsf{H}}\mathbf{A})^{-1}\mathbf{A}^{\mathsf{H}}\right]\mathbf{d}_\theta. \quad (11)$$

In (11), $\mathbf{d}_\theta = \mathrm{d}\mathbf{a}(\theta)/\mathrm{d}\theta$ is the derivative of $\mathbf{a}$ and $\mathbf{I}$ is the identity matrix. For uncorrelated signals, $\mathbf{R}_{ss}$ is diagonal, and (10) simplifies to

$$\mathrm{var}\left(\hat{\theta}_k\right) = \frac{1}{2\,N\,\mathrm{SNR}_k}\left(1 + \frac{\left[\left(\mathbf{A}^{\mathsf{H}}\mathbf{A}\right)^{-1}\right]_{kk}}{\mathrm{SNR}_k}\right)\frac{1}{\mathbf{h}(\theta_k)}, \quad (12)$$

where $\mathrm{SNR}_k = [\mathbf{R_{ss}}]_{kk}/\sigma^2$. This closed-form error estimate in (12) provides a performance benchmark for the Hankel-matrix-based single-snapshot MUSIC.

III. NUMERICAL RESULTS

We consider $M = M_0 + M_1 = 40$ antenna elements in a ULA configuration. $M_0 = 20$ high-resolution and $M_1 = 20$ 1-bit ADCs are used for mixed-ADC allocations. The inter-element spacing equals $\lambda/2$. Creating the Hankel matrix involves segmenting the original MUSIC, overlapping and dividing it into multiple segments, each of length $L + 1$, corresponding to the snapshots in the classical MUSIC algorithm. The choice of L becomes a trade-off between effective resolution, separability of the snapshot-MUSIC, and the reliability of subspace vectors. In our empirical approach, following the insights of [22], we opt for a parameter L that transforms the Hankel matrix into a quasi-square form, resulting in superior performance. For our specific study, we set L to 20, creating a Hankel matrix $\mathbf{H} \in \mathbb{C}^{21\times 20}$ that closely approximates a square matrix, and s, i.e., the number of potential sources, is set to 10.

We consider six different ADC allocations. The first two allocations are exclusive high-resolution and 1-bit ADCs cases,

(1) only high-resolution ADCs: $\delta_m = 1$ for $m \in \{1, \ldots, M\}$
(2) only 1-bit ADCs: $\delta_m = 0$ for $m \in \{1, \ldots, M\}$

and the remaining ones are mixed-ADC allocations

(3) left-edge-assigned 1-bit ADCs: $\delta_m = 0$ for $m \in \{1, \ldots, 20\}$ and $\delta_m = 1$ else
(4) right-edge-assigned 1-bit ADCs: $\delta_m = 0$ for $m \in \{21, \ldots, 40\}$ and $\delta_m = 1$ else.
(5) edge-assigned 1-bit ADCs: $\delta_m = 0$ for $m \in \{1, \ldots, 10\} \cup \{31, \ldots, 40\}$ and $\delta_m = 1$ else
(6) center-assigned 1-bit ADCs: $\delta_m = 0$ for $m \in \{11, \ldots, 30\}$ and $\delta_m = 1$ else,

where the 1-bit ADCs are located at the right or left edges exclusively, or the half of the ADCs at each edge, or in the center of the array.

III-A. RMSE, CRB, and MUSIC Error Variance

First, the performance of the single-snapshot MUSIC algorithm in a single target scenario is investigated using the theoretical CRB, Monte Carlo simulations, and an analytical approach for the MUSIC error variance. Fig. 1 illustrates the root mean square error (RMSE) in degrees for four mixed-ADC allocations and the exclusive cases of high-resolution or 1-bit ADCs across various SNRs. The RMSE is calculated based on the difference between the estimated and true DOAs. The simulations are based on 200 Monte Carlo runs spanning SNRs from -10 to 30 dB with a 5 dB interval. The horizontal axis denotes the SNR, while the vertical axis represents the RMSE in degrees. The angle searching grid has a width of 10^{-4} deg and $\theta \in [-90, 90]$. The designated target DOA, θ_{target}, is set at 10 deg.

All allocations result in a similar CRB, but the exclusive high-resolution ADC allocation results in the lowest CRB, and the exclusive 1-bit ADC allocation results in the highest CRB. The simulations show that the high-resolution ADC allocation achieves the best performance for the RMSE, followed by the allocation using the 1-bit ADCs at the left edge of the antenna array, especially for high SNRs. The remaining allocations perform similarly for high SNRs. The performance of the 1-bit allocation varies with the SNR. The worst RMSE is achieved by the allocation where the 1-bit ADCs are used at the edges of the array. As outlined in Section II-B, we present a closed-

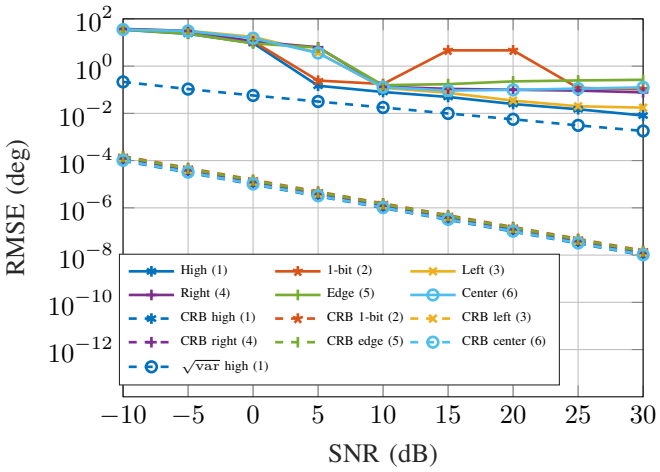

Fig. 1: RMSEs, CRBs, and error variance for different SNRs and ADC allocations using single-snapshot MUSIC.

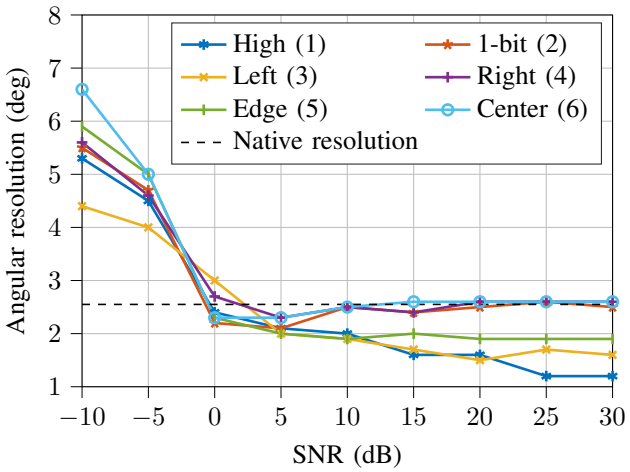

Fig. 2: Angular resolution for different SNRs and ADC allocations using single-snapshot MUSIC.

form theoretical performance benchmark, i.e., $\sqrt{\mathrm{var}\left(\hat{\theta}_i\right)}$, for MUSIC. Compared to the CRB, the Hankel-matrix-based snapshot MUSIC estimator generally exhibits a higher error magnitude. Notably, the RMSE of the high-resolution allocation closely approaches the theoretical lower error bound under conditions of sufficiently high SNR. This phenomenon arises from the inherent presence of certain errors within the estimated noise space, as specified in (7) of our single-snapshot MUSIC methodology. Further, the impact of quantization errors introduced by 1-bit ADCs is illustrated in Fig. 1, showcasing a noteworthy increase in angle estimation errors, particularly in good SNR scenarios.

III-B. Angular Resolution

Second, the angular resolution capability of single snapshot MUSIC is evaluated in a two-target scenario. Fig. 2 depicts the target separability performance for the allocations across different SNRs. The horizontal axis denotes the SNR in the -10 to $30\,\mathrm{dB}$ range with $5\,\mathrm{dB}$ spacing. The vertical axis shows the angular resolution in degrees. In the scenario, two targets with equal power are closely spaced, and their separability is assessed. The angle of the first target θ_1 is fixed to $10\,\mathrm{deg}$, while the angle θ_2 of the second target varies. The search grid width in single snapshot-MUSIC for the separability is $0.1\,\mathrm{deg}$. The native angular resolution (i.e. $3\,\mathrm{dB}$ beamwidth) is $\Delta\theta = 0.89\lambda/D$, where $D = M\,d$ is the virtual aperture length. The resolution is the minimum angle difference at which two targets are distinguishable by two peaks in the pseudospectrum $\mathbf{P}(\boldsymbol{\theta})$. With $d = \lambda/2$, the native angular resolution $\Delta\theta$ is approximately $2.55\,\mathrm{deg}$ for 40 antenna elements.

In the ULA with mixed ADCs, the target separability strongly depends on the 1-bit-ADC allocation and decreases with an increasing SNR. The allocations (1), (3), and (5) achieve a resolution below $2\,\mathrm{deg}$ for SNR values greater than $5\,\mathrm{dB}$. The high-resolution ADCs allocation performs best, especially for SNRs greater than $25\,\mathrm{dB}$. Allocation (3) has the second-best performance for an SNR greater than $10\,\mathrm{dB}$. This result is comparable to the RMSE, where the left-edge-assigned ADCs also achieved the best performance of the mixed-ADCs for large SNRs. Allocations (2), (4), and (6) achieve a resolution that is approximately equal to the native resolution of approximately $2.5\,\mathrm{deg}$. In this scenario, the 1-bit ADC allocation achieves a resolution similar to the right-edge and center allocations.

IV. CONCLUSIONS

This paper presents a novel approach for high-resolution DOA estimation in automotive radar systems using single snapshot MUSIC with mixed ADC configurations. By leveraging the Hankel matrix and SVD, we derive a pseudospectrum to identify DOAs of targets. Extensive simulations compare the RMSE of various mixed-ADC setups with the theoretical CRB and closed-form MUSIC performance benchmark. We also assess target separability across different ADC allocations. Notably, simulations favor an assignment placing 1-bit ADCs at the array's left edge. However, high-resolution ADCs consistently outperform other configurations. While our study uses fixed ADC allocations, future research could explore methods to optimize them for single snapshot MUSIC DOA estimation. Additionally, analytical performance analysis is planned to corroborate our simulated findings.

V. REFERENCES

[1] S. Sun, A. P. Petropulu, and H. V. Poor, "MIMO radar for advanced driver-assistance systems and autonomous driving: Advantages and challenges," *IEEE Signal Process. Mag.*, vol. 37, no. 4, pp. 98–117, 2020.

[2] S. Sun and Y. D. Zhang, "4D automotive radar sensing for autonomous vehicles: A sparsity-oriented approach," *IEEE J. Sel. Topics Signal Process.*, vol. 15, no. 4, pp. 879–891, 2021.

[3] Texas Instruments, "AWR1243 single-chip 77- and 79-GHz FMCW transceiver," datasheet, 2017.

[4] M. Kahlert, T. Fei, C. Tebruegge, and M. Gardill, "Doppler Ambiguity Resolution for a PMCW Automotive Radar System," in *2023 20th European Radar Conference (EuRAD)*, 2023, pp. 73–76.

[5] R. Schmidt, "Multiple emitter location and signal parameter estimation," *IEEE transactions on antennas and propagation*, vol. 34, no. 3, pp. 276–280, 1986.

[6] R. Roy and T. Kailath, "ESPRIT-estimation of signal parameters via rotational invariance techniques," *IEEE Transactions on acoustics, speech, and signal processing*, vol. 37, no. 7, pp. 984–995, 1989.

[7] W. Roberts, P. Stoica, J. Li, T. Yardibi, and F. Sadjadi, "Iterative adaptive approaches to MIMO radar imaging," *IEEE J. Sel. Topics Signal Process.*, vol. 4, no. 1, pp. 5–20, 2010.

[8] T. Yardibi, J. Li, P. Stoica, M. Xue, and A. Baggeroer, "Source localization and sensing: A nonparametric iterative adaptive approach based on weighted least squares," *IEEE Trans. Aerosp. Electron. Syst.*, vol. 46, no. 1, pp. 425–443, 2010.

[9] T. T. Cai and L. Wang, "Orthogonal matching pursuit for sparse signal recovery with noise," *IEEE Trans. Inf. Theory*, vol. 57, no. 7, pp. 4680–4688, 2011.

[10] Y. Yu, A. P. Petropulu, and H. V. Poor, "MIMO radar using compressive sampling," *IEEE J. Sel. Topics Signal Process.*, vol. 4, no. 1, pp. 146–163, 2010.

[11] ——, "Measurement matrix design for compressive sensing-based MIMO radar," *IEEE Trans. Signal Process.*, vol. 59, no. 11, pp. 5338–5352, 2011.

[12] Y. Yu, S. Sun, R. N. Madan, and A. P. Petropulu, "Power allocation and waveform design for the compressive sensing based MIMO radar," *IEEE Trans. Aerosp. Electron. Syst.*, vol. 50, no. 2, pp. 898–909, 2014.

[13] W. Liao and A. Fannjiang, "MUSIC for single-snapshot spectral estimation: Stability and super-resolution," *Applied and Computational Harmonic Analysis*, vol. 40, no. 1, pp. 33–67, 2016.

[14] G. K. Papageorgiou, M. Sellathurai, and Y. C. Eldar, "Deep networks for direction-of-arrival estimation in low SNR," *IEEE Transactions on Signal Processing*, vol. 69, pp. 3714–3729, 2021.

[15] R. Zheng, H. Liu, S. Sun, and J. Li, "Deep learning based computationally efficient unrolling IAA for direction-of-arrival estimation," in *2023 31st European Signal Processing Conference (EUSIPCO)*, 2023, pp. 730–734.

[16] R. Zheng, S. Sun, H. Liu, H. Chen, and J. Li, "Interpretable and efficient beamforming-based deep learning for single snapshot DOA estimation," *IEEE Sensors Journal*, pp. 1–1, 2023.

[17] X. Zhang, Y. Cheng, X. Shang, and J. Liu, "Optimal Mixed-ADC Arrangement for DOA Estimation Via CRB Using ULA," in *ICASSP 2023 - 2023 IEEE International Conference on Acoustics, Speech and Signal Processing (ICASSP)*, 2023, pp. 1–5.

[18] A. Papoulis, *Probability, Random Variables and Stochastic Processes (4th ed.)*. Boston, MA, USA: McGraw-Hill, 2002.

[19] I. E. Berman and T. Routtenberg, "Resource Allocation and Dithering of Bayesian Parameter Estimation Using Mixed-Resolution Data," *IEEE Transactions on Signal Processing*, vol. 69, pp. 6148–6164, 2021.

[20] X. Zhang, Y. Cheng, X. Shang, and J. Liu, "Optimal Mixed-ADC Arrangement for DOA Estimation Via CRB Using ULA," in *ICASSP 2023 - 2023 IEEE International Conference on Acoustics, Speech and Signal Processing (ICASSP)*, 2023, pp. 1–5.

[21] P. Stoica and A. Nehorai, "MUSIC, maximum likelihood, and Cramer-Rao bound," *IEEE Transactions on Acoustics, Speech, and Signal Processing*, vol. 37, no. 5, pp. 720–741, 1989.

[22] Y. Sun, T. Fei, and N. Pohl, "A high-resolution framework for range-doppler frequency estimation in automotive radar systems," *IEEE Sensors Journal*, vol. 19, no. 23, pp. 11 346–11 358, 2019.